Stochastic based compact model to predict highly variable electrical characteristics of organic CBRAM devices

Silvana Guitarra, P. Mahato, D. Deleruyelle, L. Raymond, L. Trojman

Stochastic based compact model to predict highly variable electrical characteristics of organic CBRAM devices

S. Guitarra[a,1], P. Mahato[b], D. Deleruyelle[b], L. Raymond[c], L. Trojman[a,d]

[a] *Universidad San Francisco de Quito, Colegio de Ciencias e Ingeniería, IMNE, Diego de Robles s/n-Cumbayá, Quito 170901, Ecuador*

[b] *Univ Lyon, INSA Lyon, ECL, CNRS, UCBL, CPE Lyon, INL, UMR5270, 69621 Villeurbanne, France*

[c] *Aix Marseille Université, Université de Toulon, CNRS, CPT, Marseille, France*

[d] *ISEP -Institut Supérieur d'Électronique de Paris, 10 rue de Vanves, Issy les Moulineaux, 92130-France*

Abstract

A compact model using a stochastic approach is developed in this work to capture the essential resistive switching behavior of conductive-bridge random access memory (CBRAM) device featuring a solid polymer electrolyte consisting of Polyethylene Oxide (PEO). This model considers the statistical distribution of five electrical parameters used to describe the resistive switching observed in experimental data. A switching probability is defined to control the change of resistive state. This approach gives the model the stochastic behavior of current-voltage characteristics observed in this kind of devices. A good agreement between the simulation and the experimental curves is observed despite the unusual variability cycle-to-cycle for this type of ReRAM.

Keywords: Conductive-bridge random access (CBRAM), Stochastic model, switching probability, Polyethylene oxide (PEO).

1. Introduction

Conductive-bridge random access (CBRAM) memory is a promising candidate for future nonvolatile memory device applications, thanks to its characteristics [1][2]. The resistive switching between Low Resistive State (LRS) and High Resistive State (HRS) is based on the formation and dissolution of a conductive filament by applying an appropriate voltage. However, like other ReRAM devices, they suffer from cycle-to-cycle switching variability, which is intrinsic in nature and is attributed to ion generation and migration. This behavior makes it difficult to characterize its electrical parameters for technology assessment and predict its operation [3]. Some models with different approaches have been developed in the literature to simulate its resistive switching [4][5].

Recently, a compact model based on the stochastic behavior of the ReRAM was successfully applied to HfO_2 based OXRAM [6]. This model considers a statistical distribution of the electrical parameters and the physics behind the electrical conduction phenomenon. Since the stochastic behavior is observed in any type of ReRAM, in this work, we demonstrate that this model can also be employed to predict the IV behavior of polymer based CBRAM devices.

2. Samples and experiment

CBRAMs with Polyethylene oxide (PEO) as solid polymer electrolyte (SPE) layer were fabricated with a crossbar area of 30 x 30 μm^2 on a silicon substrate. The top (Ag) and bottom (Pt) electrodes were deposited using PVD technique, while the SPE layer was deposited by spin coating [7]. The current-voltage characteristics were measured in air at room temperature using a semiconductor parameter analyzer (Keithley 4200-SCS) under DC sweep with steps of 10mV. For set process, the voltage sweep was from 0 to 2V, with a compliance current of 100 µA (Fig. 1), while for the reset, it was from 0 to -1V. The I-V curves shown in Fig. 1 were consistent with typical ReRAM butterfly curves [8].

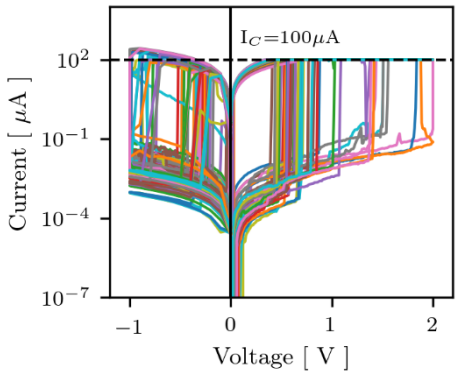

Figure. 1 Current-voltage characteristics for 100 cycles. We define V_{set} the switching voltage from HRS to LRS and V_{reset} from LRS to HRS.

It is worth noting that these IV curves showed a more significant cycle-to-cycle variability than OXRAM [6], likely related to both local PEO thickness fluctuations and random formation and disruption of the microscopic

[1]Corresponding author
Email address: sguitarra@usfq.edu.ec (Silvana Guitarra)

conductive-bridging filaments (CB) formed in the PEO layer as reported in [9][10].

3. Model applied to CBRAM

Like OXRAMs, CBRAM devices are simple Metal-Insulating-Metal (MIM) structures. Their electrical behavior relies on the reversible formation/dissolution of a metallic-rich conductive bridge (CB) [11] analog to the conductive filament (CF) of the OXRAM that are composed of different paths of oxygen vacancies [12]. In these PEO-based CBRAM devices, the cell is in LRS when Ag-rich filaments connect both electrodes, while in HRS when they are broken [13]. Further, as reported in [14], the conductive filaments have a conical shape with the narrowest region near the dielectric/inert electrode interface. In both OXRAM and CBRAM, the process of filaments growth and rupture is difficult to control, which produces variability of the filament's conduction properties observed in the IV curves.

Based on the similarities in the resistive switching mechanism between OXRAM and CBRAM, the model proposed in [6] is applied to conductive bridge samples. This model describes the filament's constricted region by a circuit composed of N-parallel branches composed of electrical elements connected in series [Fig. 2(a)], where one of these elements works as a switch between two conductance states. In LRS these switches are LR elements, while in HRS they become HR elements. The definition of the nodes and voltages associated with the model are illustrated in Fig. 2(b). The change of the inner breaker's state is determined from the applied external voltage (V_{ext}).

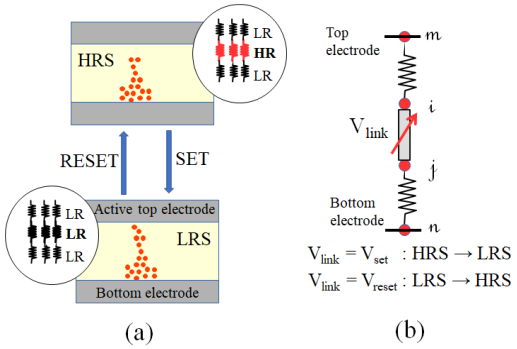

Figure. 2: (a) Scheme of the model for the resistive switching in CBRAM devices and (b) the electrical branches representation where V_{link} is the voltage drop at the breaker terminals.

When the system is in a given state (HRS or LRS), V_{ext} is applied, and the voltage drop across the breaker is computed by $V_{link} = V_i - V_j$, where i and j are the nodes of the chains (see Fig. 2b). When V_{link} is closer to V_{set} (or V_{reset}), the change of state is determined according to a switching probability, P_s, given by:

$$P_S = \frac{1}{2}\{1 + tanh[C_S(V_{link} - V_{ref})]\} \quad (1)$$

where V_{ref} is equal to V_{set} or V_{reset}, according to the process. C_s is the probability function slope and is obtained from the variability of the experimental threshold voltages $\left(C_s = \frac{1}{\sigma}\right)$. It implies that an important variability will generate smaller $|C_s|$ values that broader the probability of change. In simulation, P_s is compared with a computer-generated random number p, and only if P_s is bigger than p, the breaker state is changed. The model simulation routine is summarized in Fig. 3.

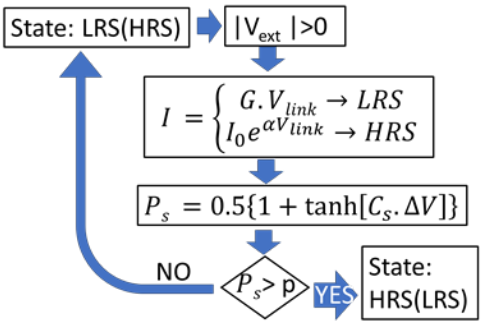

Figure. 3: Flowchart used in simulation for set (reset) process. P_s is the probability function and $\Delta V = V_{link} - V_{set(reset)}$. Once all elements in the active region are LR (or HR), the CBRAM will be in LRS (or HRS). The subindexes "s" stands for set or reset

4. Calibration

Five parameters have been extracted from experimental IV curves to describe the resistive switching of CBRAM. All of them fluctuate from cycle to cycle, which is the result of the random formation and disruption of the microscopic conductive-bridging filaments (CB) formed in the PEO layer, as reported in [9][10]. For calibration, statistical analysis of these parameters was performed.

V_{set} and V_{reset} data distributions were extracted from the experimental data (Fig. 1) to obtain the mean value (μ) and the standard deviation (σ). After, the C_s value was determined for set and reset processes (Fig. 4. and Fig. 5). These parameters are essential to calibrate the P_s function (Eq. 1) that controls the breaker´s state´s change and gives the model the stochastic behavior of the physically resistive switching. As a result, P_s includes in the model the IV variability observed in most of CBRAM devices.

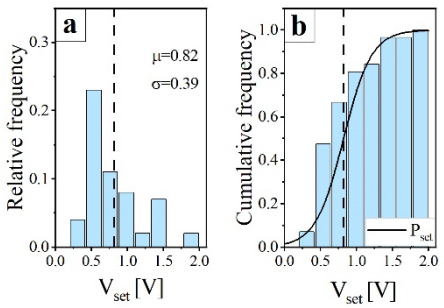

Figure. 4: Set voltage distribution follows a normal law (a). The dispersion σ = 1/C_s in the probability function (Fig. 3) consistent with the slope of P_{set} in (b).

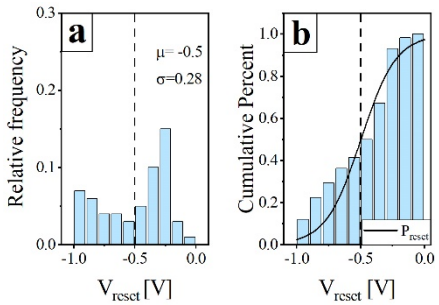

Figure. 5: Reset voltage distribution follows a normal law (a). The dispersion $\sigma = 1/C_s$ in the probability function (Fig. 3) consistent with the slope of P_{reset} in (b).

The other three parameters are related to the conduction mechanisms. When the system is in LRS, the CB connects the Ag to Pt electrodes in the polymer electrolyte. Then, the conduction could be considered ohmic, defined by:

$$I = G\,V \qquad (2)$$

where G is the CB conductance. Otherwise, in HRS the CB filaments are broken, and the conduction can be attributed to a tunnel effect transport, as derived in QPC model [15] and given by:

$$I = I_o\, e^{\alpha V} \qquad (3)$$

where I_o and α are two parameters to be obtained from experimental data. In some kinds of resistive switching devices, QPC model can explain the transition from tunneling mechanism in the HRS to Ohmic conduction in LRS [16]. However, it has been determined that in Ag\PEO\Pt devices, the Poole-Frenkel conduction mechanism is prevalent in the HRS [7]. According to that, under high electric field, the trap´s energy of barrier is lowered enough so that the electron probability of jumping to the successive trap increases. This conduction type will be included in a consecutive work.

Average values of the conduction parameters (G, I_0, and α) were obtained by fitting the I-V curves (Fig.1) to calibrate Eq. 2 and Eq. 3, taking into account to separate the LRS (Fig. 6) and HRS (Fig. 7) regime for specific voltage bias.

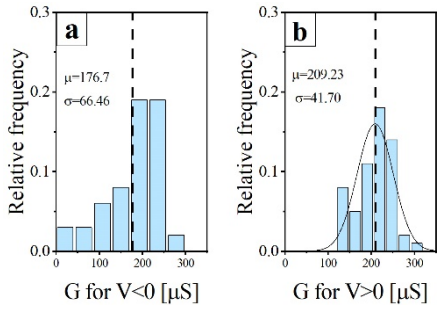

Figure. 6: Ohmic Conductance (I=GV) distribution during LRS under negative (a) and positive voltages (b).

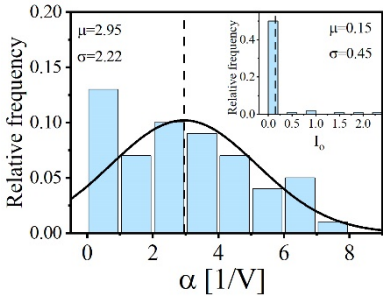

Figure. 7: Quantum Conductance [4] distribution during HRS ($I = I_o\, e^{\alpha V_{link}}$).

To obtain V_{link}, the values of V_i and current I through the system are computed by solving Kirchhoff's equations at each node of the CB filament [Fig. 2(b)]. At each step of V_{ext}, the current I was compared with the compliance current, such as occurs during measurements.

Finally, the switching probability P_s is computed and compared with a computer-generated random number *p*, and only if P_s is bigger than *p*, the breaker changes its state. When all active region elements are activated (or deactivated), the CBRAM changes its state.

The model has been implemented in a Python-based script, and it can be adapted to work with other kinds of conduction mechanisms. Previously it was successfully applied in OXRAM devices [6].

5. Simulation result and discussion

All the parameters used to calibrate the model (Fig. 3) are summarized in Table I. Fig. 8 reports the experimental data, along with simulation results. A good agreement is obtained between the simulated and experimental curves, while a high variability is highlighted for these CBRAM samples.

TABLE 1: Calibration parameters

Parameter	Value
V_{set} [V]	0.82±0.39
V_{reset} [V]	- 0.50±0.28
G [mS]	290.23±41.70
I_o [mA]	0.14±0.43
α [1/V]	2.48±2.21

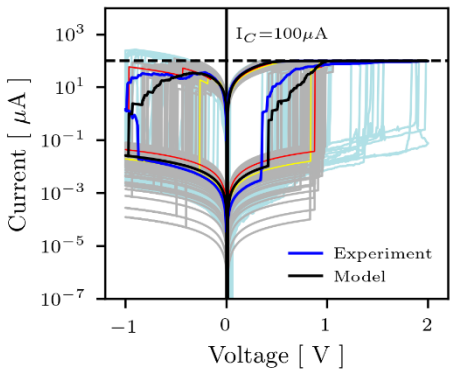

Figure. 8: Simulation results along with experimental data

The variability observed in IV curves is a common characteristic of OXRAM and CBRAM devices, and it is attributed to the stochastic nature of the switching process. However, the V_{set} and V_{reset} statistical variation is more critical in CBRAM, which implies that the transition between LRS to HRS, or vice versa, does not always occur at a particular voltage and makes them unpredictable. The PEO-CBRAM studied in this work suggests that Ag ions in the PEO polymer matrix might alternate in controlling the resistive transition [9][10]. On the other hand, the OXRAMs variability is attributed to the geometric variations of the main conductive filament [17].

This model includes the variability observed in experimental data through the statistical analysis of the electrical behavior. **Notice that there are two types of variability: device-to-device variability, associated with the CF characteristics, and the cycle-to-cycle variability, attributed to non-uniformities in the fabrication process [18]. This work is focused mainly on the first one, but it could be extended to analyze the other one.**

Finally, using more samples should improve these statistical studies and increase the simulation accuracy of the model results.

6. Conclusion

In this work, we demonstrated that the compact model considering the stochastic behavior of the ReRAM is a powerful tool to predict I-V characteristics. More specifically, we proposed a simple model that has now been validated for CBRAMs, as it was for OXRAMs, because both are based on CF. A more significant number of samples would have increased the agreement, already good, between the simulation and the experimental curves. Finally, this model can be adapted to include other kinds of conduction mechanisms and/or work with different devices that show stochastic behavior.

References

[1] Song S, Cho B, Kim TW, Ji Y, Jo M, Wang G, et al. Three-dimensional integration of organic resistive memory devices. Adv Mater 2010;22:5048–52. https://doi.org/10.1002/adma.201002575.

[2] Michael N Kozicki and Hugh J Barnaby. Conductive bridging random access memory materials, devices and applications. Semicond Sci Technol 2016;31:113001.

[3] Molas G, Sassine G, Nail C, Alfaro Robayo D, Nodin J-F, Cagli C, et al. (Invited) Resistive Memories (RRAM) Variability: Challenges and Solutions . ECS Trans 2018;86:35–47. https://doi.org/10.1149/08603.0035ecst.

[4] Yu S, Wong HP. Compact Modeling of Conducting-Bridge. IEEE Trans Electron Devices 2011;58:1352–60.

[5] Zhao YD, Hu JJ, Huang P, Yuan F, Chai Y, Liu XY, et al. A physics-based compact model for material- and operation-oriented switching behaviors of CBRAM. Tech Dig - Int Electron Devices Meet IEDM 2017:7.6.1-7.6.4. https://doi.org/10.1109/IEDM.2016.7838370.

[6] Guitarra S, Raymond L, Trojman L. Stochastic multiscale model for HfO2-based resistive random access memories with 1T1R configuration. Solid State Electron 2021;176:107947.

[7] Mahato P, Puyoo E, Deleruyelle D, Pruvost S. CBRAM devices with a water casted solid polymer electrolyte for flexible electronic applications. 2019 IEEE 14th Nanotechnol Mater Devices Conf NMDC 2019 2019;2019-Janua. https://doi.org/10.1109/NMDC47361.2019.9083996.

[8] Ielmini D, Milo V. Physics-based modeling approaches of resistive switching devices for memory and in-memory computing applications. J Comput Electron 2017;16:1121–43. https://doi.org/10.1007/s10825-017-1101-9.

[9] Celano U, Goux L, Belmonte A, Opsomer K, Detavernier C, Jurczak M, et al. Conductive filaments multiplicity as a variability factor in CBRAM. IEEE Int Reliab Phys Symp Proc 2015;2015-May:MY111–3. https://doi.org/10.1109/IRPS.2015.7112813.

[10] Krishnan K, Aono M, Tsuruoka T. Kinetic factors determining conducting filament formation in solid polymer electrolyte based planar devices. Nanoscale 2016;8:13976–84. https://doi.org/10.1039/c6nr00569a.

[11] Celano U, Goux L, Belmonte A, Opsomer K, Degraeve R, Detavernier C, et al. Understanding the Dual Nature of the Filament Dissolution in Conductive Bridging Devices. J Phys Chem Lett 2015;6:1919–24.

[12] Waser R, Dittmann R, Staikov C, Szot K. Redox-based resistive switching memories nanoionic mechanisms, prospects, and challenges. Adv Mater 2009;21:2632–63. https://doi.org/10.1002/adma.200900375.

[13] Seung HM, Kwon KC, Lee GS, Park JG. Flexible conductive-bridging random-access-memory cell vertically stacked with top Ag electrode, PEO, PVK, and bottom Pt electrode. Nanotechnology 2014;25. https://doi.org/10.1088/0957-4484/25/43/435204.

[14] Celano U, Goux L, Belmonte A, Opsomer K, Franquet A, Schulze A, Detavernier C, Richard O, Bender H, Jurczak M VW. Three-dimensional observation of the conductive filament in nanoscaled resistive memory devices. Nano Lett 2014;14:2401–6. https://doi.org/10.1021/nl500049g.

[15] Prócel LM, Trojman L, Moreno J, Crupi F, Maccaronio V, Degraeve R, et al. Experimental evidence of the quantum point contact theory in the conduction mechanism of bipolar HfO2-based resistive random access memories. J Appl Phys 2013;114. https://doi.org/10.1063/1.4818499.

[16] Lian X, Long S, Cagli C, Buckley J, Miranda E, Liu M. Conduction in Resistive Switching Memories 2012;1:101–4.

[17] Fantini A, Goux L, Degraeve R, Wouters DJ, Raghavan N, Kar G, et al. Intrinsic switching variability in HfO2 RRAM. 2013 5th IEEE Int Mem Work IMW 2013 2013:30–3.

https://doi.org/10.1109/IMW.2013.6582090.

[18] Zahoor, F., Azni Zulkifli, T.Z. & Khanday, F.A. Resistive Random Access Memory (RRAM): an Overview of Materials, Switching Mechanism, Performance, Multilevel Cell (mlc) Storage, Modeling, and Applications. *Nanoscale Res Lett* **15,** 90 (2020). https://doi.org/10.1186/s11671-020-03299-9